Knockout of the Golgi stacking proteins GRASP55 and GRASP65 impairs Golgi structure and function

Michael E. Bekier, II[a,†], Leibin Wang[a,†], Jie Li[a], Haoran Huang[a], Danming Tang[a], Xiaoyan Zhang[a], and Yanzhuang Wang[a,b,*]

[a]Department of Molecular, Cellular and Developmental Biology, University of Michigan, Ann Arbor, MI 48109-1048;
[b]Department of Neurology, School of Medicine, University of Michigan, Ann Arbor, MI 48109

ABSTRACT **Golgi reassembly stacking protein of 65 kDa (GRASP65) and Golgi reassembly stacking protein of 55 kDa (GRASP55) were originally identified as Golgi stacking proteins; however, subsequent GRASP knockdown experiments yielded inconsistent results with respect to the Golgi structure, indicating a limitation of RNAi-based depletion. In this study, we have applied the recently developed clustered regularly interspaced short palindromic repeats (CRISPR)/Cas9 technology to knock out GRASP55 and GRASP65, individually or in combination, in HeLa and HEK293 cells. We show that double knockout of GRASP proteins disperses the Golgi stack into single cisternae and tubulovesicular structures, accelerates protein trafficking, and impairs accurate glycosylation of proteins and lipids. These results demonstrate a critical role for GRASPs in maintaining the stacked structure of the Golgi, which is required for accurate posttranslational modifications in the Golgi. Additionally, the GRASP knockout cell lines developed in this study will be useful tools for studying the role of GRASP proteins in other important cellular processes.**

Monitoring Editor
Benjamin S. Glick
University of Chicago

Received: Feb 21, 2017
Revised: Aug 7, 2017
Accepted: Aug 9, 2017

INTRODUCTION

The Golgi apparatus is an essential organelle composed of stacks of tightly aligned flattened cisternal membranes, which are often laterally linked into a ribbonlike structure located in the perinuclear region of mammalian cells (Ladinsky *et al.*, 1999). The Golgi resides at the center of the secretory pathway, receiving almost the entire output of the endoplasmic reticulum (ER), including proteins and lipids that are modified and processed in the Golgi in a variety of ways, such as *N*- or *O*-linked glycosylation (Kornfeld and Kornfeld, 1985; Zhang and Wang, 2016), phosphorylation (Capasso *et al.*, 1989; Wang *et al.*, 2005b), lipidation (Gusarova *et al.*, 2007), and proteolytic cleavage (Capasso *et al.*, 1989; Kayed *et al.*, 2003). Cargo molecules maturing through the Golgi membranes are inevitably sorted and transported to their final destinations, such as the plasma membrane, endosomes, lysosomes, or secretory granules, in a precise manner for cells to maintain homeostasis (Bravo *et al.*, 1994; Shorter and Lindquist, 2004).

Formation of the unique, stacked morphology of the Golgi is controlled in part by two homologous peripheral membrane proteins, Golgi reassembly stacking protein of 65 kDa (GRASP65) and of 55 kDa (GRASP55), which are localized to the *cis*- and *medial-trans* cisternae, respectively (Barr *et al.*, 1997; Shorter *et al.*, 1999). In interphase cells, GRASP proteins form homodimers and *trans*-oligomers from adjacent cisternae to hold Golgi cisternae together to form a stack (Wang *et al.*, 2003; Xiang and Wang, 2010). GRASP proteins are also implicated in Golgi ribbon formation by linking individual Golgi stacks, likely through bridging proteins (Feinstein and Linstedt, 2008; Tang *et al.*, 2016). Interestingly, the Golgi apparatus

This article was published online ahead of print in MBoC in Press (http://www.molbiolcell.org/cgi/doi/10.1091/mbc.E17-02-0112) on August 16, 2017.

The authors declare no conflicts of interest.

†These authors contributed equally to this work.

Author contributions: M.B., L.W., and Y.W. designed the project; M.B., L.W., J.L., H.H., and X.Z. performed the experiments; L.W., M.B., H.H., and J.L. analyzed the data; L.W., M.B., and Y.W. wrote the paper.

*Address correspondence to: Yanzhuang Wang (yzwang@umich.edu.)

Abbreviations used: BSA, bovine serum albumin; CRISPR, clustered regularly interspaced short palindromic repeats; EM, electron microscope; EndoH, endoglycosidase; FACS, fluorescence-activated cell sorting; GRASP55, Golgi reassembly stacking protein of 55 kDa; GRASP65, Golgi reassembly stacking protein of 65 kDa; MAA, Maackia amurensis lectin; PBS, phosphate-buffered saline; RNAi, RNA interference; sgRNA, single-guide RNA; TGN, *trans*-Golgi network; VSV-G, vesicular stomatitis virus G protein; WGA, wheat germ agglutinin.

undergoes a unique disassembly and reassembly process during the cell cycle, which is regulated by phosphorylation of the GRASP proteins (Jesch *et al.*, 2001; Wang *et al.*, 2005a; Xiang and Wang, 2010). On mitotic entry, Cdk1 and several other kinases are activated and phosphorylate GRASP proteins (Vielemeyer *et al.*, 2009; Tang *et al.*, 2012), which impair GRASP oligomerization, resulting in Golgi cisternal unstacking. As cells exit mitosis, GRASP proteins are dephosphorylated after Cdk1 inactivation, enabling GRASPs to oligomerize and Golgi stacks to reform (Wang and Seemann, 2011; Zhang and Wang, 2015). GRASP proteins also interact with other Golgi structural proteins to regulate the morphology of the Golgi. For instance, GRASP65 interacts with GM130 (Nakamura *et al.*, 1995; Barr *et al.*, 1998), while GRASP55 forms a complex with Golgin-45 (Short *et al.*, 2001; Barr, 2005). Both GM130 and Golgin-45 are coiled-coil golgins involved in membrane tethering and Golgi structure formation (Lowe *et al.*, 1998; Lowe *et al.*, 2000; Wong and Munro, 2014). Thus GRASPs and their interacting proteins are essential for Golgi structure formation (Wang and Seemann, 2011; Tang and Wang, 2013).

Further studies in cells using RNA interference (RNAi)-mediated depletion confirmed that knockdown of a single GRASP protein reduced the number of cisternae per stack (Sutterlin *et al.*, 2005; Xiang and Wang, 2010), an effect that was rescued by the expression of exogenous GRASP proteins (Tang *et al.*, 2010b); while simultaneous depletion of both GRASPs resulted in disorganization of the entire stack (Xiang and Wang, 2010). However, GRASP depletion also caused additional effects, and thus GRASPs have been implicated in other cellular processes, including enzyme distribution (Puthenveedu *et al.*, 2006), cargo transport (D'Angelo *et al.*, 2009), unconventional secretion (Gee *et al.*, 2011; Giuliani *et al.*, 2011), cell cycle progression (Sutterlin *et al.*, 2005), apoptosis (Cheng *et al.*, 2010), and cell migration (White *et al.*, 2010). So far it is not clear whether GRASPs possess all of these functions or whether some of the effects are caused by the disruption of the Golgi stacks when GRASPs are depleted. The exact role for GRASP55 and GRASP65, therefore, remains elusive. In this study, we have used the clustered regularly interspaced short palindromic repeats (CRISPR)/Cas9 genome editing technique (Cong *et al.*, 2013; Mali *et al.*, 2013) to create loss-of-function alleles (referred to hereafter as "knockout") of GRASP55 and GRASP65, single or in combination, to investigate their roles in Golgi structure formation and function.

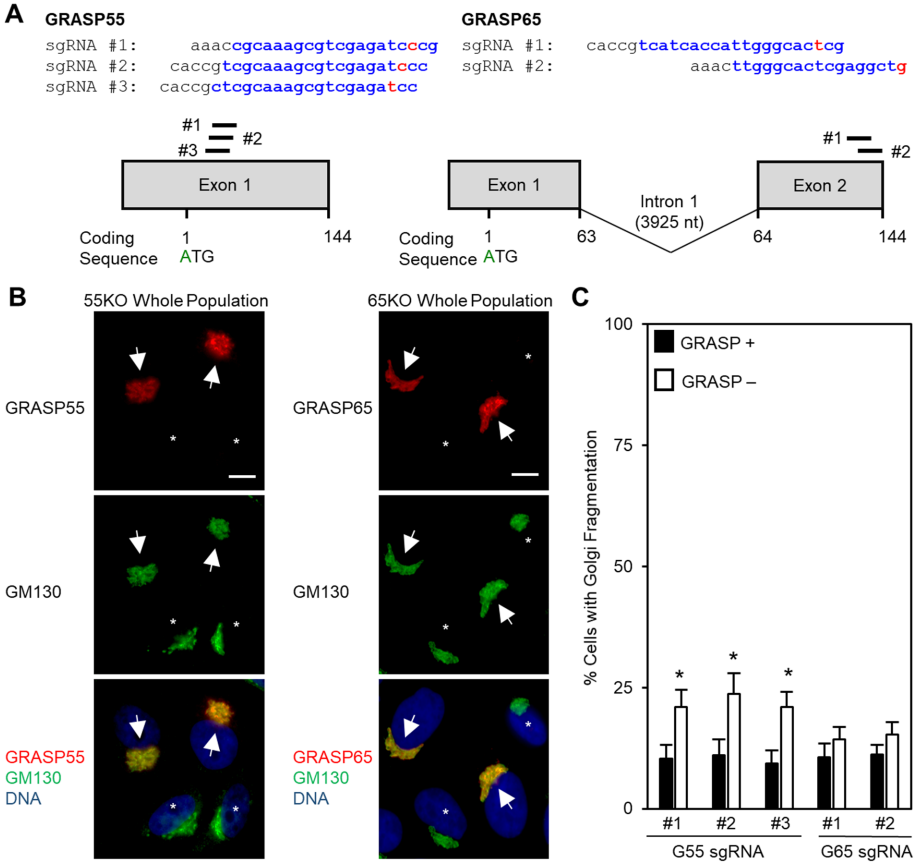

FIGURE 1: Construction of GRASP55 and GRASP65 single-knockout cells. (A) sgRNAs designed to target GRASP55 and GRASP65 using CRISPR/Cas9-mediated gene deletion. The translation initiation ATG codon is indicated and referred to as coding sequence 1 (for A); exons are indicated as boxes and introns indicated by a line, with the number of nucleotide at the splicing borders indicated. sgRNAs sequences and relative locations are indicated as lines above the exons of the gene. (B) Immunofluorescence images of cell populations transfected with sgRNAs to GRASP55 (left panels) or GRASP65 (right panels). HeLa cells were transfected with GFP-Cas9 plasmids containing sgRNAs against either GRASP55 or GRASP65 and selected for GFP expression by flow cytometry. The Golgi morphology of GRASP knockout cells was assessed by immunofluorescence microscopy for either GRASP55 or GRASP65 costained with GM130. Scale bars are 10 μm. (C) Quantification of Golgi morphology in GRASP-positive (arrows) and GRASP-negative (asterisks) cells in B. Blinded determination of the Golgi morphology of 300 cells from each sample were quantified across three biological replicates. Error bars represent SEM (Cheeseman *et al.*, 2012). A Student's *t* test was performed to determine statistical significance. *$p < 0.05$.

RESULTS

Generation of GRASP55/65 knockout HeLa and HEK293 cells

To establish GRASP55 and GRASP65 single-knockout cell lines, we designed multiple single-guide RNAs (sgRNAs) targeting exon 1 of GRASP55 (55T1, 55T2, 55T3) and exon 2 of GRASP65 (65T1, 65T2) using the target design software developed by Feng Zhang's lab at the Massachusetts Institute of Technology (http://crispr.mit.edu/) (Figure 1A). These sgRNAs all target to the coding sequences of the gene immediately downstream of the translation initiation site, and therefore no truncated proteins should be made in the cell. These sgRNAs were cloned into pSpCas9(BB)-2A-GFP(PX458) and pSpCas9(BB)-2A-Puro(PX459) vectors so positive cells could be selected by fluorescence-activated cell sorting (FACS) or by puromycin resistance. This generated a heterogeneous population of cells where ~50% of cells had no detectable levels of the target protein as determined by immunofluorescence microscopy. We then examined the morphology of the Golgi in the mixed populations of cells by immunofluorescence microscopy using GM130 as a Golgi marker. In both HeLa and HEK293 cells, GRASP65-negative cells displayed no significant changes in Golgi morphology compared with cells that expressed GRASP65 (Figure 1B and Supplemental Figure S2A). However,

GRASP55-negative cells exhibited an increased frequency of mild Golgi fragmentation compared with GRASP55-positive cells (Figure 1, B and C, and Supplemental Figures S1 and S2).

Knockout of a single GRASP protein has minor effects on the Golgi morphology

We then generated stable clones of GRASP single-knockout cells using three targets of GRASP55 (55T1, 55T2, 55T3) and two targets of GRASP65 (65T1, 65T2) in HeLa and HEK293 cells by plating selected whole populations at low density followed by clonal expansion. Multiple clones for each target were generated; consistent results were obtained in different clones generated by different sgRNAs targeting to the same gene (Supplemental Table S1). Genetic deletion of GRASP55 and GRASP65 was confirmed by genomic sequencing (Supplemental Table S2, A and B). Representative clones for each targeting sgRNA were further characterized.

Western blot analysis of GRASP55 knockout clones demonstrated that GRASP55 depletion was effective; as no GRASP55 signal was detected (Figure 2A and Supplemental Figure S3A). Knockout of GRASP55 significantly increased the level of GRASP65 in HEK293 cells (Supplemental Figure S3, A and B), although this effect was not as obvious in HeLa cells (Figure 2, A and B). GRASP55 deletion also resulted in a significant reduction of Golgin-45 in HeLa cells, while GM130 protein levels remained unchanged in both cell lines (Figure 2, A and B, and Supplemental Figure S3, A and B). Deletion of GRASP55 resulted in a minor, but significant, increase in the level of Golgi fragmentation in both HeLa and HEK293 cells, as assessed by immunofluorescence microscopy for GM130 and TGN46 (Figure 2, C–E, and Supplemental Figure S3, C–E). However, colocalization of GM130 and TGN46, as measured by Pearson's correlation coefficient, remained unchanged in HeLa cells.

Knockout of GRASP65 was also confirmed by Western blotting (Figure 3A and Supplemental Figure S4A). Interestingly, GRASP65 deletion significantly increased the protein level of GRASP55 in HeLa cells (Figure 3A), indicating that a mechanism of compensation might exist between GRASP proteins. GRASP65 deletion also reduced the level of GM130, in particular in HEK293 cells (Figure 3, A and B, and Supplemental Figure S4, A and B), consistent with previous reports (Xiang and Wang, 2010). GRASP65 knockout had no significant effects on Golgi morphology when assessed by immunofluorescence microscopy (Figure 3, C–E, and Supplemental Figure S4, C–E).

Double deletion of both GRASP55 and GRASP65 results in severe Golgi fragmentation

Deletion of GRASP55 or GRASP65 individually had only a mild impact, if at all, on the Golgi morphology when assessed by immunofluorescence microscopy. This can be explained by three possible reasons: 1) GRASP55 and GRASP65 play complementary roles in Golgi structure formation; the second GRASP protein can largely maintain the Golgi structure intact when the first one is deleted (Xiang and Wang, 2010); 2) the increased level of the other GRASP protein when its homologue is deleted may provide compensatory effect on Golgi structure formation; and 3) light microscopy does not reach the appropriate resolution to assess Golgi stack formation, and therefore the effect must be assessed by electron microscopy (EM). To address the first two possibilities, we simultaneously deleted both GRASP proteins in HeLa and HEK293 cells. Like the generation of GRASP55/65 single-knockout cells, 65T1 HeLa and HEK293 cells, instead of wild-type cells, were transfected with GRASP55 sgRNA target #2 to generate a double-knockout population and multiple, individual clones were selected (Supplemental Table S1). Deletion of both GRASP55 and GRASP65 was confirmed by Western blotting and sequencing of the genomic DNA (Figure 4A, Supplemental Figure S5A, and Supplemental Table S2, A and B). Further characterization of two representative clones demonstrated that GRASP double-knockout resulted in a significant reduction in the protein levels of both GM130 and Golgin-45 in both HeLa (Figure 4, A and B) and HEK293 cells (Supplemental Figure S5, A and B). We then assessed the Golgi morphology by immunofluorescence for GM130 and TGN46. Double knockout of GRASP proteins resulted in a dramatic dispersal of

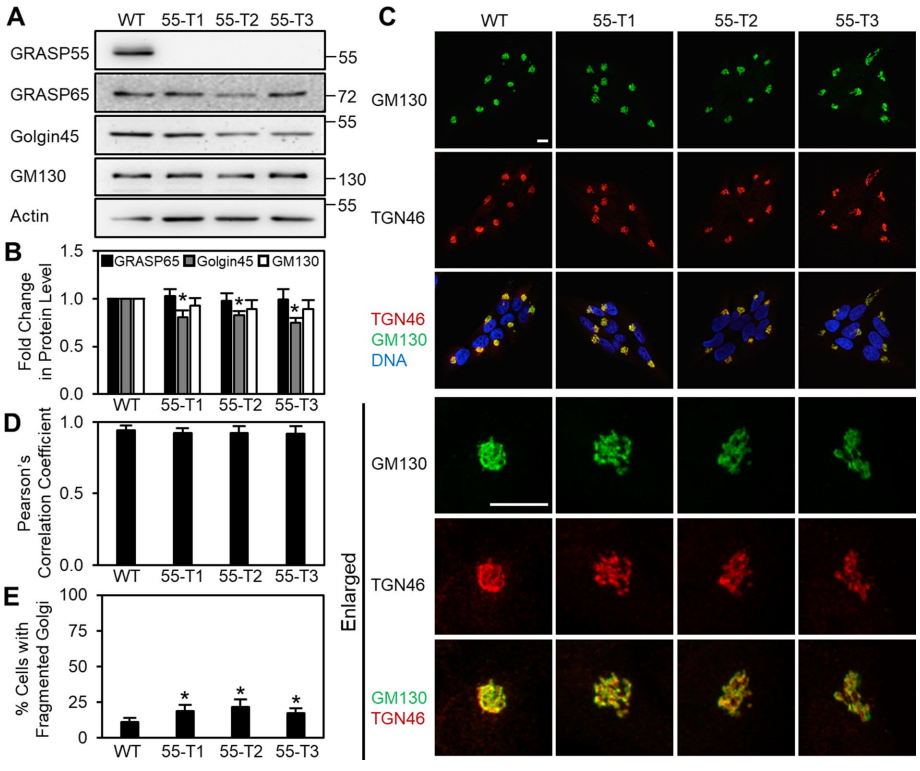

FIGURE 2: GRASP55 deletion has minor effects on the Golgi structure. (A) Western blots of Golgi proteins in GRASP55 knockout HeLa cells. Wild-type and representative GRASP55 knockout clones from three separate sgRNAs (T1, T2, and T3) were lysed and blotted for GRASP55/65, Golgin-45, and GM130. (B) Quantification of A for the relative levels of GRASP65, Golgin-45, and GM130 in GRASP55 knockout cells. Error bars represent SEM. (C) Immunofluorescence of GRASP55 knockout clones stained for GM130 and TGN46. The lower three rows are increased magnifications of the Golgi in a single cell. Scale bars are 10 μm. (D) Colocalization of GM130 and TGN46 quantified by the Pearson's correlation coefficient of z-stacks from GRASP55 knockout clones from C. Error bars represent SEM. (E) Quantification of Golgi fragmentation in GRASP55 knockout clones in C. Blinded determination of the Golgi morphology of 300 cells from each sample were quantified across three biological replicates. Error bars represent SEM. A Student's *t* test was performed to determine statistical significance. *$p < 0.05$.

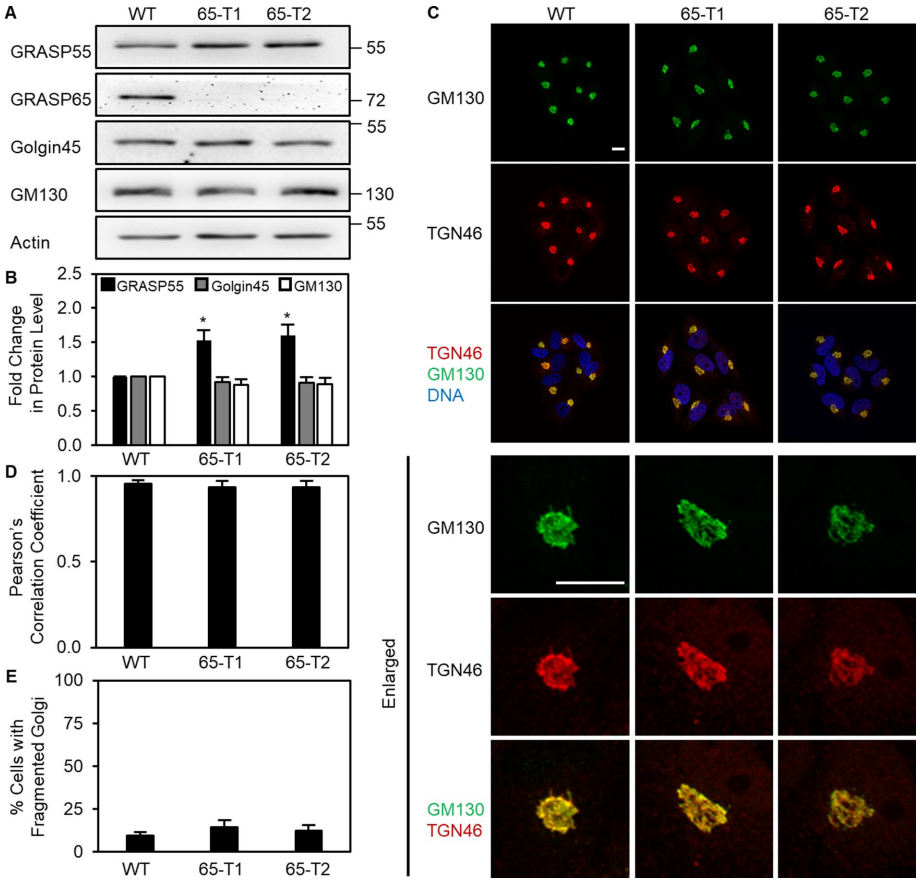

FIGURE 3: GRASP65 deletion does not cause Golgi ribbon unlinking. (A) Western blots of Golgi proteins in GRASP65 knockout HeLa cells. Wild-type and representative GRASP65 knockout clones from two separate sgRNAs (T1 and T2) were analyzed by Western blot for GRASP55/65, Golgin-45, and GM130. (B) Quantification of A for the relative levels of GRASP55, Golgin-45, and GM130 in GRASP65 knockout cells. Error bars represent SEM. (C) Immunofluorescence microscopy of GRASP65 knockout clones stained for GM130 and TGN46. The lower three rows are increased magnifications of a single cell's Golgi. Scale bars are 10 μm. (D) Colocalization of GM130 and TGN46 quantified by the Pearson's correlation coefficient of z-stacks from GRASP65 knockout clones from C. Error bars represent SEM. (E) Quantification of Golgi fragmentation in GRASP65 knockout clones in C. Blinded determination of the Golgi morphology of 300 cells from each sample were quantified across three biological replicates. Error bars represent SEM. A Student's *t* test was performed to determine statistical significance. *$p < 0.05$.

the Golgi in 95% of the HeLa cells (and ~65% in HEK293 cells) and significant decrease in the colocalization between GM130 and TGN46, indicating a disruption of Golgi stack formation (Figure 4, C–E, and Supplemental Figure S5, C–E). Furthermore, adding back of a single GRASP protein in GRASP double-knockout cells was sufficient to rescue the Golgi ribbon-linking defect observed by microscopy (Supplemental Figure S6). Overall this indicates that GRASP proteins play complementary roles in Golgi ribbon linking.

GRASP deletion impairs Golgi stacking

To more closely examine the morphology of the Golgi in GRASP single- and double-knockout cells, we performed AiryScan confocal microscopy, which significantly improves resolution compared with standard confocal microscopy (Huff, 2015). Like conventional confocal microscopy, the morphology of the Golgi in GRASP55 and GRASP65 single-knockout clones exhibited a compact Golgi ribbon and significant colocalization between GM130 and TGN46, similarly to the morphological characteristics of the Golgi in parental cells. However, the Golgi in GRASP double-knockout cells was extremely fragmented and disorganized, with a significant decrease in colocalization between GM130 and TGN46 (Figure 5A). To specify the effects of GRASP deletion on Golgi stacking, we treated WT and GRASP knockout cells with nocodazole, which is known to disassociate the Golgi ribbon into distinct Golgi stacks but does not significantly disrupt Golgi stack formation in interphase cells. On nocodazole treatment, GM130 and TGN46 colocalized in wild-type control cells, as assessed by AiryScan confocal microscopy. Deletion of a single GRASP did not significantly affect colocalization between GM130 and TGN46; however, double deletion of both GRASPs resulted in severe separation between GM130 and TGN46 (Figure 5, B and C), indicating that GRASP double knockout impairs stack formation.

To determine the ultrastructural details of the Golgi in GRASP knockout cells, we performed electron microscopy. As shown in Figure 5, D and E (galleries of images are shown in Supplemental Figure S8, A–D), depletion of a single or both GRASP proteins resulted in a higher frequency of disorganized membranes, such as short and unaligned cisternae, a reduced number of cisternae in the stack, and vesicle accumulation; the effects were more dramatic in GRASP double-knockout cells. Quantitation of the EM images showed that the ratio of disorganized membrane clusters versus distinguishable Golgi stacks in the perinuclear region of the cell was significantly increased in GRASP knockout cells compared with wild-type HeLa cells (3.5 ± 2.7% in wild-type, 43.0 ± 4.4% and 27.0 ± 2.8% in GRASP55 or GRASP65 knockout cells, respectively, and 73.2 ± 10.0% in double-knockout cells) (Figure 5, D and E). Moreover, even the distinguishable Golgi stacks in both single- and double-knockout cells did not seem to be normal, as they often contained swollen and shorter Golgi cisternae that were not properly aligned and a reduced number of cisternae per stack (Figure 5, D–H). If only well-organized Golgi stacks in the cells were quantified, then the number of organized Golgi stacks per cell was significantly reduced in GRASP55 and GRASP65 single-knockout cells (0.41 ± 0.06 and 0.55 ± 0.02, respectively) compared with control cells (2.06 ± 0.11), while almost no well-organized Golgi stacks were visible in GRASP double-knockout cells (Figure 5F). These results provide compelling evidence that GRASP55/65 are required for Golgi stack formation.

GRASP knockout accelerates protein trafficking but impairs accurate glycosylation of proteins and lipids

Previous studies showed that GRASP depletion by RNAi disrupts Golgi stack formation, which subsequently impairs accurate protein glycosylation and sorting (Xiang *et al.*, 2013). To test the effect of GRASP knockout on protein trafficking, we expressed the

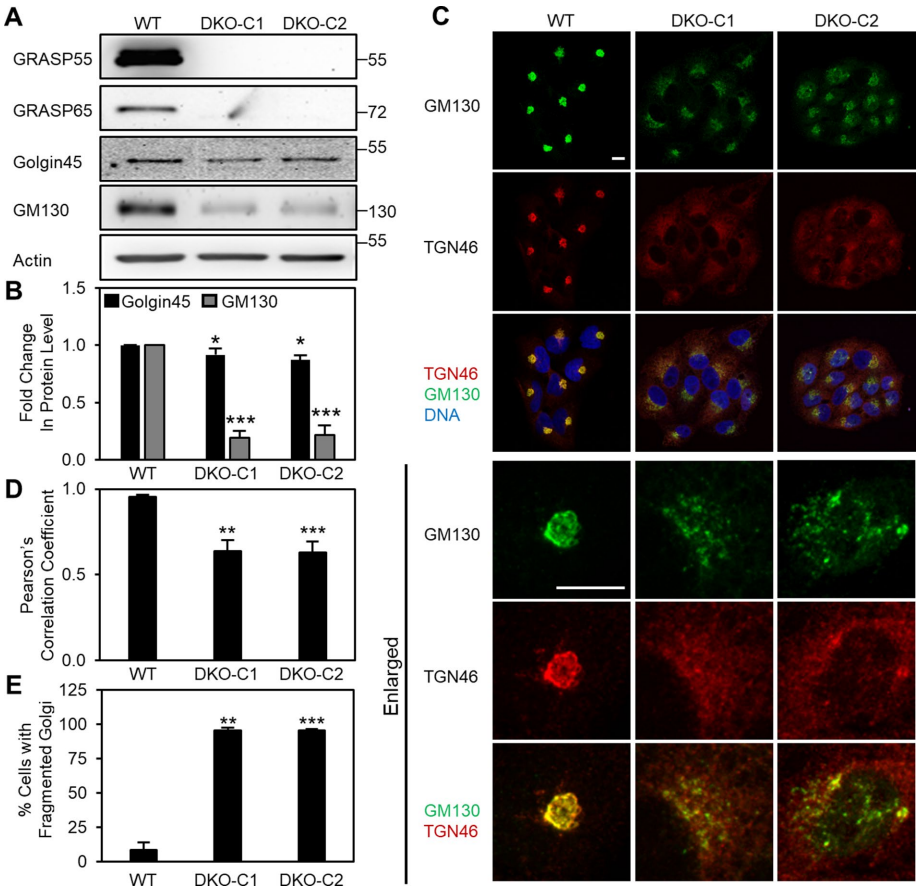

FIGURE 4: Double deletion of GRASP55 and GRASP65 results in Golgi fragmentation. (A) Western blots of Golgi proteins in GRASP55 and GRASP65 double-knockout cells. Wild-type and two representative GRASP55 and GRASP65 double-knockout clones (DKO-C1 and DKO-C2) were analyzed by Western blot for GRASP55/65, Golgin-45, and GM130. (B) Quantification of the relative levels of Golgin-45, and GM130 in GRASP double-knockout cells in A. Error bars represent SEM. (C) Immunofluorescence microscopy of GRASP55/65 double-knockout cells stained for GM130 and TGN46. The lower three rows are increased magnifications of a single cell's Golgi. Scale bars are 10 µm. (D) Colocalization of GM130 and TGN46 quantified by the Pearson's correlation coefficient of z-stacks from GRASP doubl-knockout clones from C. Error bars represent SEM. (E) Quantification of cells with fragmented Golgi from GRASP double-knockout clones in C. Blinded determination of the Golgi morphology of 300 cells from each sample were quantified across three biological replicates. Error bars represent SEM. A Student's *t* test was performed to determine statistical significance. *$p < 0.05$; **$p < 0.01$; ***$p < 0.001$.

temperature-sensitive mutant of vesicular stomatitis virus G protein (VSV-G) in cells by viral infection (Xiang *et al.*, 2013). As shown in Figure 6, A and B, single or double deletion of GRASP proteins accelerated VSV-G trafficking indicated by the increased amount of VSV-G protein that is resistant to EndoH treatment by 15 min after the temperature shift.

To test the effect of GRASP deletion on glycosylation of plasma membrane proteins, we performed cell surface staining with fluorescently labeled wheat germ agglutinin (WGA) that binds sialic acid and N-acetylglucosamine (GlcNAc), and with Maackia amurensis lectin (MAA), which binds α(2,3) sialic acid of glycans. GRASP single-knockout cells displayed a reduction in the intensity of both lectins on the cell surface; while double deletion of both GRASPs resulted in a similar effect (Figure 6, C and D). We also assessed the glycosylation pattern of two glycoproteins, Lamp1 and Lamp2, using a mobility shift assay (Xiang *et al.*, 2013). The mobility of Lamp1 and Lamp2 on SDS–PAGE was largely increased in GRASP single- and double-knockout HeLa cells, indicating a reduction in glycosylation of both Lamp1 and Lamp2 (Figure 6E). These results indicate that GRASP knockout disrupts accurate protein glycosylation for proteins both inside the cell and at the cell surface.

To determine whether GRASP deletion affects glycosylation of lipids, we stained cell surface with Shiga toxin B, which binds globotriaosylceramide (Gb3) (Jacewicz *et al.*, 1986; Ling *et al.*, 1998), and cholera toxin B, which binds monosialotetrahexosylganglioside (GM1) (Holmgren *et al.*, 1975; Merritt *et al.*, 1994). Both Gb3 and GM1 gangliosides are glycolipids synthesized in the Golgi and then transported to the cell surface. Shiga toxin cell surface stain was significantly reduced in GRASP55 knockout cells and completely abolished in both GRASP65 knockout and GRASP55/65 double-knockout cells compared with a relative strong stain of wild-type HeLa cells. Conversely, GRASP single- or double-knockout cells displayed higher levels of cholera toxin stain compared with wild-type HeLa cells (Figure 6, F–H). Importantly, the effect of GRAP depletion on Gb3 and GM1 levels at the cell surface of double-knockout cells was rescued after adding back both GRASP proteins (Supplemental Figure S7). Taken together, these results indicate that GRASP knockout enhances protein trafficking, impairs accurate glycosylation of proteins, and disrupts production and/or trafficking of glycolipids.

DISCUSSION

In this study, we have provided new evidence that GRASP55/65 play essential roles in Golgi structure formation, in particular in stacking. Knockout of a single GRASP protein reduces the number of cisternae in the stack, while double depletion of both GRASP proteins results in disorganization of the entire Golgi stack. These results are consistent with our previous results that inhibition of GRASP65 by microinjection of GRASP65 antibodies (Wang *et al.*, 2003) or by depletion of GRASP proteins by RNAi (Tang *et al.*, 2010b; Xiang and Wang, 2010) both disrupted the Golgi structure (Xiang and Wang, 2010; Xiang *et al.*, 2013). These results demonstrate that GRASP55/65 function as Golgi stacking factors.

A second function for the GRASP proteins in Golgi structure formation is to link the Golgi stacks together to form a ribbon (Puthenveedu *et al.*, 2006; Tang *et al.*, 2016). In this study, however, knocking out a single GRASP protein in either HeLa or HEK293 cells did not cause significant Golgi fragmentation at the level of immunofluorescence. Previously Lee *at al.* (2014) observed that transient knockdown of both GRASPs did not eliminate Golgi stacking. Regardless of the knockdown efficiency, the Golgi stacks are disorganized and the cisternae are not properly aligned, although the Golgi membranes are still concentrated and closely associated with each other (Lee *et al.*, 2014). We speculate that golgins and GRASPs may have different roles in Golgi structure formation: While golgins and membrane-microtubule interactions bring Golgi membranes

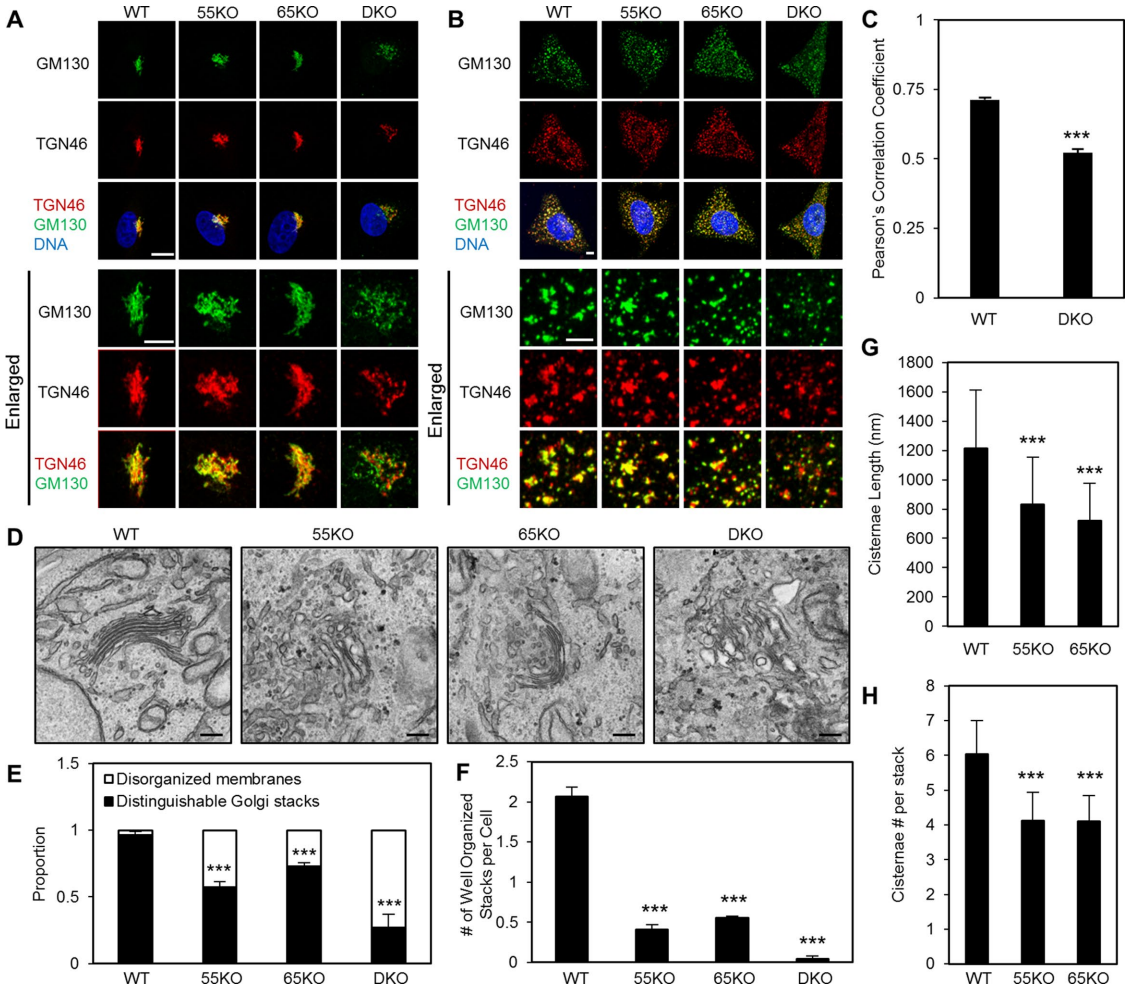

FIGURE 5: Double deletion of GRASP55 and GRASP65 proteins impairs Golgi stack formation. (A) High-resolution AiryScan confocal immunofluorescence images of GM130 and TGN46 in HeLa wild-type and GRASP single- and double-knockout clones. The lower three rows are increased magnifications of a single cell's Golgi. Scale bar is 10 μm. (B) High-resolution AiryScan confocal immunofluorescence images for GM130 and TGN46 in HeLa wild-type and GRASP single- and double-knockout clones after 4 h treatment with 100 ng/ml nocodazole. The lower three rows are increased magnifications of a single cell's Golgi. Scale bar is 5 μm. (C) Quantification of GM130 and TGN46 colocalization in B. Pearson's correlation coefficient in wild-type and GRASP55 and GRASP65 double-knockout cells from 20 cells across three biological replicates and quantified using the ImageJ2 coloc2 plug-in with z-stacks. Error bars represent SEM. A Student's *t* test was performed to determine statistical significance. (D) Electron micrographs from wild-type and GRASP single- and double-knockout HeLa clones. Note the reduced number of cisternae in GRASP single-knockout cells and the disorganized Golgi membranes in double-knockout cells. Scale bar is 200 nm. (E) Quantification of the proportion of cells exhibiting distinguishable Golgi stacks vs. disorganized membranes in D. (F) Quantification of well-organized Golgi stacks per cell in wild-type and GRASP single- and double-knockout clones from D. (G) Quantification of the length of well-organized Golgi stacks in wild-type and GRASP single-knockout clones from D. Double-knockout cells were not quantified due to the lack of well-organized stacks. (H) Quantification of the number of cisternae per stack in wild-type and GRASP single-knockout clones from D. Double-knockout cells were not quantified due to the lack of well-organized stacks. In all EM pictures, E–H, at least 20 cells across three biological replicates were quantified. Error bars represent SEM. A Student's *t* test was performed to determine statistical significance. ***$p < 0.001$.

together to the pericentriolar region, GRASPs organize them into proper stacks. Consistent with our results, this study showed that knockdown of GRASP55/65 increased CD8 trafficking (Lee *et al.*, 2014). Recently a GRASP65 knockout mouse has been reported, with only limited defects in the structure and function of the Golgi (Veenendaal *et al.*, 2014). One major concern of this knockout mouse is the potential for only partial deletion of the gene, leaving a possibility that an N-terminal 115-amino-acid fragment of GRASP65 may still be translated; this fragment is sufficient for oligomerization (Tang *et al.*, 2010b; Truschel *et al.*, 2011; Feng *et al.*, 2013), a key property essential for Golgi stacking (Wang *et al.*, 2003, 2005a). The lack of an obvious phenotype in Golgi stacking in the GRASP65 knockout mouse may also be due to the complementation by GRASP55 (Shorter *et al.*, 1999; Lee *et al.*, 2014). Taking the results together, we conclude that a complete knockout of both GRASPs is needed to further evaluate their functions. In this study, we designed multiple sgRNAs targeting to exon 1 of GRASP55 and exon 2 of GRASP65, which are directly

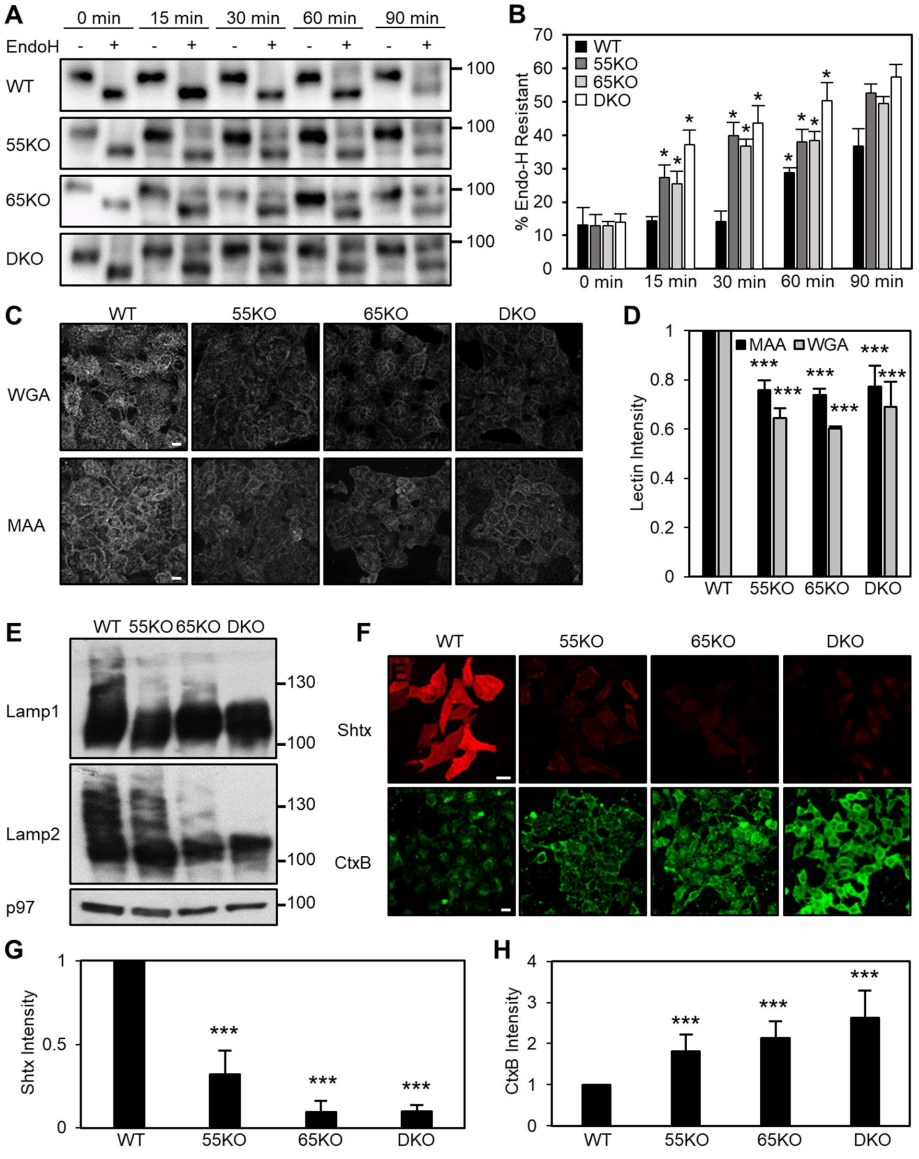

FIGURE 6: GRASP deletion accelerates protein trafficking but causes glycosylation defects. (A) GRASP deletion accelerates VSV-G trafficking. HeLa wild-type and GRASP knockout cells were infected with VSV-G-ts045-GFP adenovirus and incubated at 40.5°C for 16 h followed by cyclohexamide treatment for 1 h. Cells were then shifted to 32°C to permit trafficking of VSV-G from the ER to the plasma membrane through the Golgi. Cells were collected at the indicated time points, treated with endoglycosydase H (Endo-H), and analyzed by Western blot for GFP. Note that GRASP deletion increased VSV-G Endo-H resistance by the 15-min time point. (B) Quantification of the percentage of Endo-H resistant (upper band) VSV-G from A. (C) GRASP deletion reduces the amount of sialic acid modifications on the cell surface. Wild-type and indicated GRASP knockout HeLa cells were stained with WGA or MAA lectin without permeabilization. Note the reduced WGA and MAA intensity on GRASP knockout cells. (D) Flow cytometric analysis of WT and GRASP knockout HeLa cells stained with WGA and MAA. The fluorescence intensity of 10,000 cells was determined by flow cytometry across three biological replicates. Error bars represent SEM. A Student's *t* test was used to determine statistical significance. (E) GRASP deletion reduces glycosylation of Lamp1 and Lamp2 glycoproteins. HeLa wild-type and GRASP knockout cells were analyzed by Western blots for Lamp1 and Lamp2; note their increased migration shift on the gel when GRASPs are deleted. (F) GRASP deletion impacts glycolipids at the cell surface. Wild-type and indicated GRASP knockout HeLa cells were stained with Shiga toxin B (Shtx) or cholera toxin B (CtxB) without permeabilization. Note the reduced ShTx intensity but increased CtxB intensity in GRASP knockout cells. (G) Quantitation of cell-surface ShTx intensity from cells in F. (H) Quantification of cell-surface cholera toxin from cells in F. For G and H, the mean intensity of 200 cells from each condition was quantified in maximum projections across three biological replicates. Error bars represent SEM. A Student's *t* test was performed to determine statistical significance. $*p < 0.05$; $***p < 0.001$.

downstream of the first ATG for translation initiation. Treatment of cells with these sgRNAs resulted in either insertions or deletions that caused a frame shift of the gene with an immediate stop codon, as confirmed by DNA sequencing of individual clones (Supplemental Table S2). This ensures that no functional, truncated proteins are generated in the cell lines. Analysis of these cells with light and electron microscopy demonstrated that double-deletion of both GRASPs completely disrupted Golgi stack formation and ribbon linking. On the basis of these results and previous literature, we conclude that stacking is the primary function of GRASP proteins.

GRASP depletion also accelerates protein trafficking and disrupts glycosylation of cell surface proteins. These results are consistent with our previous study with GRASP depletion by RNAi (Xiang *et al.*, 2013). A plausible explanation for this finding is that when Golgi cisternae are fully stacked, vesicles can form and fuse only at the peripheral area of the cisternae; once the cisternae are unstacked, more membrane area becomes accessible, thereby increasing the rate of vesicle budding and cargo transport through the Golgi (Wang *et al.*, 2008; Wang and Seemann, 2011). In support of this, an in vitro budding assay has consistently demonstrated that unstacking increased the rate of coat protein complex I (COPI) vesicle formation from Golgi membranes (Wang *et al.*, 2008). GRASP proteins have also been implicated in cell cycle control (Sutterlin *et al.*, 2002). In this study, we did not observe significant change in cell growth or apoptosis, similar to GRASP knockdown (Xiang *et al.*, 2013), although more careful characterization of cell growth in these cell lines is needed in the future. GRASP depletion also altered the glycolipid profile on the cell surface. This could be due to either a shift in the production of GM1 and Gb3 or due to a defect in trafficking. Further characterization of glycolipid trafficking and production in GRASP depleted cells is clearly warranted.

An interesting observation we have made in this study is that when one GRASP protein was deleted, the level of the other GRASP protein often increased. For example, when GRASP65 was deleted, the GRASP55 protein level increased by 1.6-fold (Figure 3). These results reveal an autonomous regulatory mechanism in maintaining the Golgi integrity and function. That is, not only GRASP55 and GRASP65 play complementary roles in Golgi stack formation and function, but also the total amount of GRASP proteins in the cell might

be also regulated and therefore the total force to hold Golgi cisternae into stacks remains consistent. The nature of this mechanism, including the regulation of GRASP mRNA and protein synthesis and regulation by cellular metabolic activities, as well as GRASP targeting and degradation, will be interesting future topics of this study.

In conclusion, we have generated GRASP55 and GRASP65 single- and double-knockout HeLa and HEK293 cells. Characterization of these cell lines demonstrated that GRASP55 or GRASP65 single-knockout partially impaired Golgi cisternal stacking, whereas double-knockout of both GRASP proteins disassembled the entire Golgi structure. Furthermore, disassembly of the Golgi structure not only accelerated protein trafficking but also impaired accurate glycosylation of cell surface proteins and lipids. These cell lines provide useful tools to study the mechanism and biological significance of Golgi structure formation and could potentially be used to study the pathology of diseases in which the Golgi is defective, such as Alzheimer's disease (Nakagomi *et al.*, 2008; Joshi *et al.*, 2014), congenital disorders of glycosylation (Willett *et al.*, 2013), foot-and-mouth disease (Zhou *et al.*, 2013), reoxygenation injury (Li *et al.*, 2016), and cancer (Petrosyan, 2015).

MATERIALS AND METHODS

Reagents, plasmids, and antibodies

All reagents were purchased from Sigma-Aldrich, Invitrogen, Roche, Calbiochem, and Fisher unless otherwise stated. Antibodies used in this study include monoclonal antibodies against LAMP1 (H4A3; Developmental Studies Hybridoma Bank [DSHB]), LAMP2 (H4B4; DSHB), integrin β1 (P5D2; DSHB), integrin α-5 (BIIG2; DSHB), Shiga toxin B (A42L; Thermo-Fisher), and β-actin (Sigma); polyclonal antibodies against GRASP55 (ProteinTech), GRASP65 (UT465; Joachim Seemann, UT Southwestern), GM130 (N73; Joachim Seemann, UT Southwestern), Golgin-45 (ProteinTech), TGN46 (Bio-Rad), and GFP (Santa Cruz). Vesicular stomatitis virus G protein (VSV-G)-GFP adenovirus was a gift from David Sheff (University of Iowa) and Heike Fölsch (Northwestern University). The pUC19 plasmid was a gift from Daniel Klionsky (University of Michigan). pSpCas9(BB)-2A-GFP(PX458), pSpCas9(BB)-2A-Puro (PX459) plasmids are from Addgene. Other materials used in this study include the following: tetramethylrhodamine (TRITC)-WGA (EY laboratories), TRITC-MAA (EY laboratories), fluorescein isothiocyanate (FITC)-cholera toxin B subunit (C1655, Sigma), Shiga toxin type 1 Subunit B (NR-860, BEI Resources), and puromycin (Thermo-Fisher).

CRISPR-Cas9 knockout of GRASP genes

Guide RNA sequences targeting the GRASP55 and GRASP65 genetic loci were designed using the MIT Zhang Lab sgRNA Design Tool (crispr.mit.edu). Duplexed sgRNA oligos purchased from Invitrogen were digested and ligated into pSpCas9(BB)-2A-GFP(PX458) and pSpCas9(BB)-2A-Puro(PX459) to generate GRASP55/65 GFP or Puro plasmids, respectively. CRISPR knock-out cells were generated by transfection with GRASP55/65 GFP or Puro plasmids followed by enrichment of GFP-expressing cells by FACS sorting or by selection with 1 μg/ml puromycin, respectively. Individual clones were generated by plating cells at low density and isolating individual colonies. GRASP knockout was confirmed by Western blotting, immunofluorescence, and DNA sequencing. For sequencing of GRASP55 and GRASP65, genomic loci were amplified by PCR using the following primers:

GRASP55 (5′-CGCGGATCCTGGTGTGTGTTGAGTTCGCT-3′, 3′-CCCAAGCTTCTCCAGCCCGTCCTCCTA-5′). GRASP65 (5′-CGCGGATCCTCTAGAGCAGCATTCCCACAG-3′, 3′-CCCAAGCTTGATGGGCCAAGGTAGTGGATG-5′).

PCR products were cloned into pUC19, and the DNA sequence of 10–20 clones from each cell line was determined by Sanger Sequencing at the University of Michigan DNA Sequencing Core using M13Rev standard sequencing primer. The sequencing results are aligned with NCBI Reference Sequences of GRASP55 (NM_015530.4) and GRASP65 (NC_000003.12).

Immunofluorescence microscopy

Immunofluorescence was performed as described previously (Wang *et al.*, 2005a; Tang *et al.*, 2010a). Briefly, HeLa and HEK293 cells were fixed in 4% paraformaldehyde (PFA) in phosphate-buffered saline (PBS) for 15 min followed by quenching with 50 mM NH_4Cl in PBS for 10 min and permeabilization with 0.1% Triton X-100 in PBS for 10 min. Permeabilized cells were blocked with 2% bovine serum albumin (BSA) in PBS for 1 h followed by incubation with primary antibodies for 1.5 h, washed with PBS, and incubated with secondary antibodies for 45 min at room temperature. DNA was stained with Hoechst (1 μg/ml), and coverslips were mounted with Moviol. Widefield fluorescence microscopy was performed on a Zeiss Observer Z1 using a 63×/1.4 oil objective at a Z-step of 0.5 μm. Standard confocal microscopy was performed on a Leica SP5 using a 63×/1.4 oil objective at a 400-Hz scan rate in a 512 × 512 scan field with a Z-step of 0.5 μm. Airyscan confocal images were collected using an LSM 880 confocal system outfitted with an Airyscan detector (Carl Zeiss, Jena, Germany) to optimize resolution of fixed cell preparations. Briefly, multitrack acquisition was performed with 405-, 488-, and 633-nm wavelengths using a Plan-Apochromat 63×/1.4 oil objective. Images were scanned with a pixel scaling of 37 nm in XY with a Z-step of 144 nm. Resulting emission was centered on a 32-element GaAsP-based spatial detector, and channels were reassigned to a central GaAsP element to effectively reduce imaging volumes from 1.25 Airy units to 0.2 Airy units. This reassignment step was performed via the ZEN software (Carl Zeiss) using a recommended Wiener filter parameter for weighing noise in given images. Final images were assessed against confocal (nonAiryscan) images to ensure artifact-free improvements in resolution and signal to noise.

Electron microscopy

EM was performed as previously described (Tang *et al.*, 2010a). Briefly, cells were plated in six-well dishes. After 24 h of culture, cells were fixed with 2.5% glutaraldehyde and then processed for Epon embedding. Sections of 60 nm were mounted onto Formvar-coated nickel grids and double contrasted with 2% uranyl acetate for 5 min and 3% lead citrate for 5 min. Grids were imaged using a Philips CM100 Biotwin and JEOL JEM-1400 transmission electron microscope. EM images were taken from the perinuclear region of the cell where Golgi membranes were normally concentrated. Golgi stacks and Golgi clusters were identified using morphological criteria and quantitated using standard stereological techniques. For HeLa wild-type and GRASP knockout cells, the profiles had to contain a nuclear profile with an intact nuclear envelope. A cisterna was defined as a membrane-bound structure in the Golgi cluster whose length is at least 4 times its width, normally 20–30 nm in width and longer than 150 nm (Lucocq *et al.*, 1989), and a stack is the set of flattened, disk-shaped cisternae resembling a stack of plates. Multiple unstacked cisternae and vesicles were counted as disorganized membrane clusters, whereas stacked structures with two or more cisternae were counted as distinguishable Golgi stacks and only stacked structures with well aligned, smooth, normal-length cisternae were counted as well-organized Golgi stacks.

Lectin staining

Lectin staining was performed as previously described (Willett *et al.*, 2013). In short, cells were grown on coverslips to 70% confluency then incubated with ice-cold PBS for 15 min followed by fixation with 1% PFA for 15 min and quenching with 50 mM NH_4Cl for 10 min. Cells were then washed three times with PBS and blocked in 1% BSA in PBS for 30 min at room temperature. After blocking, cells were incubated with fluorophore-conjugated lectins for 30 min at room temperature followed by three 10-min PBS washes and mounted onto glass slides. The following lectins (and working concentrations) were used: TRITC-WGA (2 µg/ml) and TRITC-MAA (20 µg/ml).

Fluorescence-activated cell sorting

Flow cytometry analysis for lectin staining was performed as previously described (Bailey Blackburn *et al.*, 2016). In short, cells were grown to 70% confluency and then incubated with ice-cold PBS for 15 min followed by treatment with 20 mM EDTA for 5 min. Cells were collected after treatment with 20 mM EDTA for 5 min and resuspended in 0.1% BSA/PBS. After blocking on ice for 30 min, cells were incubated with fluorophore-conjugated lectins in 0.1% BSA with indicated concentration for 30 min while shaking on ice followed by washing with ice-cold PBS. Cells were then fixed with 1% PFA for 15 min and quenched with 50 mM NH_4Cl for 10 min before submitted for flow cytometry. Cells were analyzed using the LSRFortessa (BD Biosciences) flow cytometer gated for correct cell size versus complexity and fluorescence intensity. Analysis was done using FCS Express 6 software. Fluorescence intensity was quantified from 10,000 cells from three replicates. Statistical significance was determined by performing a two-tier Student's *t* test.

VSV-G trafficking assay

VSV-G trafficking assay was performed as previously described (Xiang *et al.*, 2013). Briefly, cells were plated in 3.5-cm dishes and cultured overnight. Subsequently the medium was removed and serum-free medium was added that contained VSV-G-ts045-GFP adenovirus. Following a 2 h incubation with the virus, the VSV-G–containing medium was removed, and cells were grown in full medium at 40.5°C for 16 h. Cells were then treated with 0.1 mM cycloheximide for 1 h prior to shifting the temperature to 32°C. Cells were harvested at the indicated time points, and an Endo-H assay was performed.

Shiga toxin and cholera toxin binding assay

Shiga toxin and cholera toxin assay were performed as previously described (Selyunin and Mukhopadhyay, 2015). In short, for Shiga toxin binding assay, cells were plated onto coverslips and cultured overnight. Cells were then washed three times with cold PBS and incubated with 4 µg/ml purified Shiga toxin 1B subunit in cold medium for 30 min on ice. After being washed three times with ice-cold PBS, cells were fixed with 4% PFA and quenched with 50 mM NH_4Cl, followed by subsequent incubation with an anti-Shiga toxin B primary antibody for 1.5 h and secondary antibody for 1.5 h at room temperature. DNA was stained with Hoechst. Coverslips were mounted with Moviol. Images were taken on a Leica SP5 confocal microscope.

For cholera toxin binding, cells were plated onto coverslips and cultured overnight. Cells were washed three times with ice-cold PBS and incubated with 4 µg/ml FITC-conjugate cholera toxin B subunit in cold media for 30 min on ice. Cells were then washed three times with ice-cold PBS and fixed with 4% PFA, quenched with 50 mM NH_4Cl, and stained for DNA with Hoechst. Images were taken on a Leica SP5 confocal microscope.

For the addback experiment, GRASP double-knockout cells were transfected with GRASP55-mCherry and either GRASP65-myc (cholera toxin assay) or GRASP65-GFP (Shiga toxin assay). Cells were processed as previously described but with minor alterations to the cholera toxin assay protocol to enable visualization of exogenously expressed GRASP proteins and toxin labelling. Briefly, after toxin binding and fixation, cells were subject to permeabilization with 0.1% Triton X-100 in PBS and blocking in 1% BSA in PBS followed by immunofluorescence using a myc antibody.

Quantification and statistics

In all figures, the quantification results are expressed as the mean ± SEM from three independent experiments, unless otherwise stated. The statistical significance of the results was assessed using a two-tailed Student's *t* test. For quantitation of VSV-G trafficking, a one-tailed Student's *t* test was used to determine statistical significance; $*p < 0.05$; $**p < 0.01$; $***p < 0.001$ in all figures.

ACKNOWLEDGMENTS

We thank Kamlesh Bisht and Jayakrishnan (J.K.) Nandakumar (University of Michigan) for technical support on the CRISPR technique, Joachim Seemann for antibodies, and David Sheff and Heike Fölsch for VSV-G ts045-GFP adenovirus. We thank other members of the Wang lab for suggestions, reagents, and technical support. This work was supported in part by National Institutes of Health Grant GM112786, MCubed, and the Fast Forward Protein Folding Disease Initiative of the University of Michigan to Y. W.

REFERENCES

Bailey Blackburn J, Pokrovskaya I, Fisher P, Ungar D, Lupashin VV (2016). COG complex complexities: detailed characterization of a complete set of HEK293T cells lacking individual COG subunits. Front Cell Dev Biol 4, 23.

Barr FA (2005). Purification and functional interactions of GRASP55 with Rab2. Methods Enzymol 403, 391–401.

Barr FA, Nakamura N, Warren G (1998). Mapping the interaction between GRASP65 and GM130, components of a protein complex involved in the stacking of Golgi cisternae. EMBO J 17, 3258–3268.

Barr FA, Puype M, Vandekerckhove J, Warren G (1997). GRASP65, a protein involved in the stacking of Golgi cisternae. Cell 91, 253–262.

Bravo DA, Gleason JB, Sanchez RI, Roth RA, Fuller RS (1994). Accurate and efficient cleavage of the human insulin proreceptor by the human proprotein-processing protease furin. Characterization and kinetic parameters using the purified, secreted soluble protease expressed by a recombinant baculovirus. J Biol Chem 269, 25830–25837.

Capasso JM, Keenan TW, Abeijon C, Hirschberg CB (1989). Mechanism of phosphorylation in the lumen of the Golgi apparatus: translocation of adenosine 5′-triphosphate into Golgi vesicles from rat liver and mammary gland. J Biol Chem 264, 5233–5240.

Cheeseman LP, Booth DG, Hood FE, Prior IA, Royle SJ (2012). Aurora A kinase activity is required for localization of TACC3/ch-TOG/clathrin inter-microtubule bridges. Commun Integr Biol 4, 409–412.

Cheng JP, Betin VM, Weir H, Shelmani GM, Moss DK, Lane JD (2010). Caspase cleavage of the Golgi stacking factor GRASP65 is required for Fas/CD95-mediated apoptosis. Cell Death Dis 1, e82.

Cong L, Ran FA, Cox D, Lin S, Barretto R, Habib N, Hsu PD, Wu X, Jiang W, Marraffini LA, Zhang F (2013). Multiplex genome engineering using CRISPR/Cas systems. Science 339, 819–823.

D'Angelo G, Prencipe L, Iodice L, Beznoussenko G, Savarese M, Marra P, Di Tullio G, Martire G, De Matteis MA, Bonatti S (2009). GRASP65 and GRASP55 sequentially promote the transport of C-terminal valine bearing cargoes to and through the golgi complex. J Biol Chem 284, 34849–34860.

Feinstein TN, Linstedt AD (2008). GRASP55 regulates Golgi ribbon formation. Mol Biol Cell 19, 2696–2707.

Feng Y, Yu W, Li X, Lin S, Zhou Y, Hu J, Liu X (2013). Structural insight into Golgi membrane stacking by GRASP65 and GRASP55 proteins. J Biol Chem 288, 28418–28427.
Gee HY, Noh SH, Tang BL, Kim KH, Lee MG (2011). Rescue of DeltaF508-CFTR trafficking via a GRASP-dependent unconventional secretion pathway. Cell 146, 746–760.
Giuliani F, Grieve A, Rabouille C (2011). Unconventional secretion: a stress on GRASP. Curr Opin Cell Biol 23, 498–504.
Gusarova V, Seo J, Sullivan ML, Watkins SC, Brodsky JL, Fisher EA (2007). Golgi-associated maturation of very low density lipoproteins involves conformational changes in apolipoprotein B, but Is not dependent on apolipoprotein E. J Biol Chem 282, 19453–19462.
Holmgren J, Lönnroth I, Månsson J, Svennerholm L (1975). Interaction of cholera toxin and membrane GM1 ganglioside of small intestine. Proc Natl Acad Sci USA 72, 2520–2524.
Huff J (2015). The Airyscan detector from ZEISS: confocal imaging with improved signal-to-noise ratio and super-resolution. Nat Meth 12.
Jacewicz M, Clausen H, Nudelman E, Donohue-Rolfe A, Keusch G (1986). Pathogenesis of shigella diarrhea. XI. Isolation of a shigella toxin-binding glycolipid from rabbit jejunum and HeLa cells and its identification as globotriaosylceramide. J Exp Med 163, 1391–1404.
Jesch SA, Lewis TS, Ahn NG, Linstedt AD (2001). Mitotic phosphorylation of Golgi reassembly stacking protein 55 by mitogen-activated protein kinase ERK2. Mol Biol Cell 12, 1811–1817.
Joshi G, Chi Y, Huang Z, Wang Y (2014). Abeta-induced Golgi fragmentation in Alzheimer's disease enhances Abeta production. Proc Natl Acad Sci USA 111, E1230–1239.
Kayed R, Head E, Thompson JL, McIntire TM, Milton SC, Cotman CW, Glabe CG (2003). Common structure of soluble amyloid oligomers implies common mechanism of pathogenesis. Science 300, 486–489.
Kornfeld R, Kornfeld S (1985). Assembly of asparagine-linked oligosaccharides. Ann Rev Biochem 54, 631–664.
Ladinsky MS, Mastronarde DN, McIntosh JR, Howell KE, Staehelin LA (1999). Golgi structure in three dimensions: functional insights from the normal rat kidney cell. J Cell Biol 144, 1135–1149.
Lee I, Tiwari N, Dunlop MH, Graham M, Liu X, Rothman JE (2014). Membrane adhesion dictates Golgi stacking and cisternal morphology. Proc Natl Acad Sci USA 111, 1849–1854.
Li T, You H, Mo X, He W, Tang X, Jiang Z, Chen S, Chen Y, Zhang J, Hu Z (2016). GOLPH3 bediated Golgi stress response in modulating N2A cell death upon oxygen-glucose eeprivation and reoxygenation Injury. Mol Neurobiol 53, 1377–1385.
Ling H, Boodhoo A, Hazes B, Cummings MD, Armstrong GD, Brunton JL, Read RJ (1998). Structure of the Shiga-like toxin I B-pentamer complexed with an analogue of its receptor Gb3. Biochemistry 37, 1777–1788.
Lowe M, Gonatas NK, Warren G (2000). The mitotic phosphorylation cycle of the cis-Golgi matrix protein GM130. J Cell Biol 149, 341–356.
Lowe M, Rabouille C, Nakamura N, Watson R, Jackman M, Jamsa E, Rahman D, Pappin DJ, Warren G (1998). Cdc2 kinase directly phosphorylates the cis-Golgi matrix protein GM130 and is required for Golgi fragmentation in mitosis. Cell 94, 783–793.
Lucocq JM, Berger EG, Warren G (1989). Mitotic Golgi fragments in HeLa cells and their role in the reassembly pathway. J Cell Biol 109, 463–474.
Mali P, Yang L, Esvelt KM, Aach J, Guell M, DiCarlo JE, Norville JE, Church GM (2013). RNA-guided human genome engineering via Cas9. Science 339, 823–826.
Merritt EA, Sarfaty S, van den Akker F, L'Hoir C, Martial JA, Hol WG (1994). Crystal structure of cholera toxin B-pentamer bound to receptor GM1 pentasaccharide. Prot Sci 3, 166–175.
Nakagomi S, Barsoum MJ, Bossy-Wetzel E, Sütterlin C, Malhotra V, Lipton SA (2008). A Golgi fragmentation pathway in neurodegeneration. Neurobiol Dis 29, 221–231.
Nakamura N, Lowe M, Levine TP, Rabouille C, Warren G (1997). The vesicle docking protein p115 binds GM130, a cis-Golgi matrix protein, in a mitotically regulated manner. Cell 89, 445–455.
Nakamura N, Rabouille C, Watson R, Nilsson T, Hui N, Slusarewicz P, Kreis TE, Warren G (1995). Characterization of a cis-Golgi matrix protein, GM130. J Cell Biol 131, 1715–1726.
Petrosyan A (2015). Onco-Golgi: is fragmentation a gate to cancer progression? Biochem Mol Biol J 1, 16.
Puthenveedu MA, Bachert C, Puri S, Lanni F, Linstedt AD (2006). GM130 and GRASP65-dependent lateral cisternal fusion allows uniform Golgi-enzyme distribution. Nat Cell Biol 8, 238–248.
Selyunin AS, Mukhopadhyay S (2015). A conserved structural motif mediates retrograde trafficking of Shiga toxin types 1 and 2. Traffic 16, 1270–1287.
Short B, Preisinger C, Korner R, Kopajtich R, Byron O, Barr FA (2001). A GRASP55-rab2 effector complex linking Golgi structure to membrane traffic. J Cell Biol 155, 877–883.
Shorter J, Lindquist S (2004). Hsp104 catalyzes formation and elimination of self-replicating Sup35 prion conformers. Science 304, 1793–1797.
Shorter J, Watson R, Giannakou ME, Clarke M, Warren G, Barr FA (1999). GRASP55, a second mammalian GRASP protein involved in the stacking of Golgi cisternae in a cell-free system. EMBO J 18, 4949–4960.
Sutterlin C, Hsu P, Mallabiabarrena A, Malhotra V (2002). Fragmentation and dispersal of the pericentriolar Golgi complex is required for entry into mitosis in mammalian cells. Cell 109, 359–369.
Sutterlin C, Polishchuk R, Pecot M, Malhotra V (2005). The Golgi-associated protein GRASP65 regulates spindle dynamics and is essential for cell division. Mol Biol Cell 16, 3211–3222.
Tang D, Wang Y (2013). Cell cycle regulation of Golgi membrane dynamics. Trends Cell Biol 23, 296–304.
Tang D, Xiang Y, Wang Y (2010a). Reconstitution of the cell cycle-regulated Golgi disassembly and reassembly in a cell-free system. Nat Protoc 5, 758–772.
Tang D, Yuan H, Vielemeyer O, Perez F, Wang Y (2012). Sequential phosphorylation of GRASP65 during mitotic Golgi disassembly. Biol Open 1, 1204–1214.
Tang D, Yuan H, Wang Y (2010b). The role of GRASP65 in Golgi cisternal stacking and cell cycle progression. Traffic 11, 827–842.
Tang D, Zhang X, Huang S, Yuan H, Li J, Wang Y (2016). Mena-GRASP65 interaction couples actin polymerization to Golgi ribbon linking. Mol Biol Cell 27, 137–152.
Truschel ST, Sengupta D, Foote A, Heroux A, Macbeth MR, Linstedt AD (2011). Structure of the membrane-tethering GRASP domain reveals a unique PDZ ligand interaction that mediates Golgi biogenesis. J Biol Chem 286, 20125–20129.
Veenendaal T, Jarvela T, Grieve AG, van Es JH, Linstedt AD, Rabouille C (2014). GRASP65 controls the cis Golgi integrity in vivo. Biol Open 3, 431–443.
Vielemeyer O, Yuan H, Moutel S, Saint-Fort R, Tang D, Nizak C, Goud B, Wang Y, Perez F (2009). Direct selection of monoclonal phosphospecific antibodies without prior phosphoamino acid mapping. J Biol Chem 284, 20791–20795.
Wang Y, Satoh A, Warren G (2005a). Mapping the functional domains of the Golgi stacking factor GRASP65. J Biol Chem 280, 4921–4928.
Wang Y, Seemann J (2011). Golgi biogenesis. Cold Spring Harb Perspect Biol 3, a005330.
Wang Y, Seemann J, Pypaert M, Shorter J, Warren G (2003). A direct role for GRASP65 as a mitotically regulated Golgi stacking factor. EMBO J 22, 3279–3290.
Wang Y, Taguchi T, Warren G (2005b). Purification of rat liver Golgi stacks. In: Cell Biology: A Laboratory Handbook, 3rd ed., ed. J Celis, San Diego: Elsevier Science (USA), 33–39.
Wang Y, Wei JH, Bisel B, Tang D, Seemann J (2008). Golgi cisternal unstacking stimulates COPI vesicle budding and protein transport. PLoS ONE 3, e1647.
White DT, McShea KM, Attar MA, Santy LC (2010). GRASP and IPCEF promote ARF-to-Rac signaling and cell migration by coordinating the association of ARNO/cytohesin 2 with Dock180. Mol Biol Cell 21, 562–571.
Willett RA, Pokrovskaya ID, Lupashin VV (2013). Fluorescent microscopy as a tool to elucidate dysfunction and mislocalization of Golgi glycosyltransferases in COG complex depleted mammalian cells. Methods Mol Biol 1022, 61–72.
Wong M, Munro S (2014). Membrane trafficking: the specificity of vesicle traffic to the Golgi is encoded in the golgin coiled-coil proteins. Science 346, 1256898.
Xiang Y, Wang Y (2010). GRASP55 and GRASP65 play complementary and essential roles in Golgi cisternal stacking. J Cell Biol 188, 237–251.
Xiang Y, Zhang X, Nix DB, Katoh T, Aoki K, Tiemeyer M, Wang Y (2013). Regulation of protein glycosylation and sorting by the Golgi matrix proteins GRASP55/65. Nat Commun 4, 1659.
Zhang X, Wang Y (2015). GRASPs in Golgi structure and function. Frontiers Cell Dev Biol 3, 84.
Zhang X, Wang Y (2016). Glycosylation quality control by the Golgi structure. J Mol Biol 428, 3183–3193.
Zhou Z, Mogensen MM, Powell PP, Curry S, Wileman T (2013). Foot-and-mouth disease virus 3C protease induces fragmentation of the Golgi compartment and blocks intra-Golgi transport. J Virol 87, 11721–11729.